Pergamon

European Journal of Cancer, Vol. 34, No. 1, pp. 175–181, 1998

Printed in Great Britain
0959-8049/98 $19.00+0.00

PII: S0959-8049(97)00371-7

Original Paper

The DNA Content of Chromosome Division Figures and Interphase Nuclei Classifies Ulcerative Colitis

R.G. Steinbeck

Department of Oncology and Pathology, Karolinska Institute and Hospital, S-171 76 Stockholm, Sweden

Long-standing ulcerative colitis is considered to be a precancerous condition. Therefore, a practical and reliable method is required for monitoring the progress of the disease. Liberation of the S-phase from karyokinesis occurs in DNA amplification and endoreplication, producing nuclei with more than 4 *c* DNA. The amount of Feulgen DNA was quantified with an image microphotometer in 8 μm sections for interphase nuclei and in 15 μm sections for chromosome division figures (CDFs). Development of ulcerative colitis was investigated in low grade dysplasia ($n = 93$ cases; score 3–7) and high grade dysplasia ($n = 22$; score 8–10). Bacterial colitis ($n = 34$) and invasive adenocarcinoma ($n = 26$) provided a basis for data interpretation in dysplasia. Lymphocyte nuclei served as an internal DNA standard. CDFs represent a novel type of aberrant 'mitoses'; they are different from and much more frequent than figures with multipolar spindles. Endoreplication began with low grade dysplasia in interphase nuclei as well as with CDFs; it was fully established in high grade dysplasia and carcinoma. Endoreplicated interphase nuclei and CDFs represent an early morphological mosaic of genomic instability. Both characteristics support a reproducible two-level classification of low and high grade dysplasia in ulcerative colitis. © **1997 Published by Elsevier Science Ltd.**

Key words: CDF, ulcerative colitis, endoreplication, microphotometry, tumorigenesis
Eur J Cancer, Vol. 34, No. 1, pp. 175–181, 1998

INTRODUCTION

PRECANCEROUS CONDITIONS such as ulcerative colitis demand objective and reproducible criteria for classification. Divergence in criteria and variations in observations are potential sources of errors [1]. A uniform approach to small human biopsies, fixed in formaldehyde, should guarantee effective comparison over time and geographical areas.

Cells in activated tissues or hyperplastic lesions are found not only in G_0/G_1 with 2 *c* DNA content, but also in G_2/M with 4 *c* DNA after passage through the S-phase of the mitotic cycle. The *c* value represents the (haploid) genome equivalent. By contrast, profiles from neoplastic lesions have been recorded above the 4 *c* level. The 5 *c* exceeding rate (ER) is the accepted threshold for DNA aneuploidy [2–4]. Nuclei beyond 4 *c* must be created by endoreplication when DNA synthesis occurs *in vivo* without nuclear division [5–7]. This phenomenon of genome multiplication demands the uncoupling of S-phase(s) from mitosis [8] and has also been called over-replication and re-replication. The terms endoreduplication, endomitosis or polyploidisation should be restricted to cases of pure geometric 2^n increase in chromosomal DNA [9].

The discrimination between endoreplication and endoreduplication is essential for the classification of chromosome division figures (CDFs) in precancerous and cancerous lesions of colon mucosa and oral mucosa [10]. CDFs are very similar to mitotic figures, but possess (much) more DNA than 4.0 *c*. CDFs can be morphologically addressed (*mad*-prophases, *mad*-metaphases, *mad*-telophases) and represent a novel class of "atypical mitoses" due to their amplified DNA content. There are also aberrant figures with multipolar spindles [11, 12], but they are rather rare compared to CDFs. The impact of CDFs in cancer development has been demonstrated earlier, when specimens subjected to comparative genomic hybridisation [13] were evaluated using single-cell microphotometry (unpublished data). The reliability of single-cell microphotometry in microsections has been previously established [10, 14].

Correspondence to R.G. Steinbeck, PO Box 2761, D-24917 Flensburg, Germany.
Received 20 Mar. 1997; revised 11 Jun. 1997; accepted 10 Jul. 1997.

In this study, microphotometry was used to examine cases of ulcerative colitis, because quantitative records and qualitative features can be obtained simultaneously. Thus, interphase nuclei and CDFs were measured in an accurate area of the lesion. The aim of the present investigation was to evaluate the DNA content of interphase nuclei and of CDFs against the background of histological classification established by Morson [15].

MATERIALS AND METHODS

Tissue samples

The material comprised 112 cases of ulcerative colitis with different degrees of epithelial atypia in the mucous membrane and of unknown duration. 26 further cases of colonic adenocarcinoma and 34 cases of bacterial colitis were added to study tumour progression. Adenocarcinomas were obtained from patients following hemicolectomy, while other material was obtained by endoscopic examination. Interphase nuclei from normal healthy mucosa was used as a standard. Biopsies were from patients of the Flensburg district, Northern Germany. Endogenous lymphocyte nuclei ($n = 30$) provided a 2 *c* DNA standard in each case. Furthermore, activated human lymphocytes (10, each with a normal karyotype) provided an *in vitro* system of benign hyperplasia.

Histological classification

The biopsies were fixed with buffered 4% formaldehyde (minimum 30 min) and paraffin embedded. For histological diagnosis, 4 μm sections were stained with haematoxylin and eosin. A modification of histological classification for dysplasia [15] was applied using a score system (Table 1). After summing up the scores, the histological findings were qualified as follows: no dysplasia 0–2 points, low grade dysplasia 3–7, high grade dysplasia 8–10. After DNA microphotometry, a second histological evaluation was done to find the degree of intra-observer variation.

Quantitative DNA analysis

Microphotometry was carried out by the same highly experienced operator (> 10 000 cases). The image-analysis system (Ahrens, Bargteheide, Germany) was equipped with a plan objective (40/0.95 for immersion, Nikon) and a CCD camera (Nikon). Interphase nuclei were measured in 8 μm sections; those which had been cut were avoided [16]. Each DNA profile was sampled from 150 interphase nuclei. Mitotic figures and CDFs were measured in 15 μm sections. For the Feulgen procedure, specimens were hydrolysed in one batch of 5 M HCl at 22°C for 60 min and stained in one batch of Schiff's reagent at RT for 90 min [17]. The quantitative records at 546 nm were automatically calibrated against an internal 2 *c* DNA standard (at least 20 lymphocyte nuclei) and expressed as *c* values. The reliability of measurements was based on selecting the correct tumour area and on measuring complete nuclei. These essentials were obtained by optical control and appropriate depth for interphases (8 μm) and division figures (15 μm). The coefficient of variation (c.v.) from any lymphocyte population was < 0.07, indicating high precision.

Histogram calibration

Interphase nuclei from cases of hyperplasia (e.g. the activated lymphocytes) were constantly found in the range of mitotic amounts (2–4 *c* DNA, where *c* is the haploid genome equivalent). The 2 *c* level was fixed with resting lymphocytes, and the 4 *c* level was found from cultivated lymphocytes in prophase. The nuclear DNA increased beyond 4 *c* in neoplasia. To assure this event, the 4.5 *c* exceeding rate (ER) and the 5 *c* ER were used as thresholds.

RESULTS

Interphase nuclei

Biopsies of ulcerative colitis, complicated with epithelial atypia, were classified according to criteria suggested by Morson [15]. This first histological classification of each case was carried out with a scoring list pertaining mainly to nuclear features (Table 1). Individual interphase nuclei were measured with the microphotometer and automatically sorted into three fractions. The G_0/G_1 population covered 1.8–2.4 *c* DNA content and was represented by the cells of normal healthy mucosa. Bacterial colitis (Col) and activated lymphocytes are ruled by the mitotic cycle, but the second peak was recorded in the range of 2.5–4.9 *c* because of the given software. However, nuclei > 4.4 *c* were a rare event. Definitely endoreplicated cells were identified by the 5 *c* ER. Tumour progression was characterised by a decline in diploid cells and a corresponding increase in the endoreplicated fraction (Table 2). The onset of DNA endoreplication was found with 1.9% of nuclei in low grade dysplasia, increased to 10.3% in high grade dysplasia and a final 20.5% in colonic carcinoma.

After DNA measurement of interphase nuclei, the intra-observer variation was obtained by a second histological evaluation with the same scoring list (Table 1). The second scores were plotted against the 5 *c* ER in the interphase nuclei (Figure 1). Scores concurred in 86.0% of low grade dysplasia and with 81.8% in high grade dysplasia. Disagreement occurred mainly in cases at the histological transition from low grade dysplasia to high grade dysplasia. These cases had

Table 1. *Histological classification of dysplasia in ulcerative colitis*

Low grade	Score	High grade	Score
Nuclei			
hyperchromatic	1	pronounced hyperchromatic	2
enlarged, elongated	1	prominently enlarged, rounded	2
some loss of polarity	1	general loss of polarity	2
regular mitotic figures	1	suspicious division figures	2
Tissue pattern			
slight changes, budding and branching	1	atrophy, villous pattern, polyposis, thickening of MM	2
Additional alterations			
minimal inflammation, some loss of goblet cells		no inflammation, dystrophic goblet cells	

Table 2. Frequency distribution of DNA content in interphase nuclei

Histology	(*n*)	1.8–2.4 *c* (%)	2.5–4.9 *c* (%)	5 *c* ER (%)
Normal mucosa	5	94.3 ± 1.2	5.7 ± 1.2	0
Bacterial colitis	34	85.3 ± 1.5	14.6 ± 1.5	0.1 ± 0.1
Activated lymphocytes	10	39.4 ± 2.2	60.5 ± 2.2	0.1 ± 0.1
Ulcerative colitis				
Low grade dysplasia	93	70.2 ± 0.9	27.9 ± 0.8	1.9 ± 0.2
High grade dysplasia	19	49.4 ± 6.3	40.3 ± 4.5	10.3 ± 2.5
Colon adenocarcinoma	26	7.4 ± 3.0	72.1 ± 3.9	20.5 ± 3.8

150 nuclei were measured at random in each case. Sections 8 μm thick. Numerical scattering given as ± SEM. *c*, genome equivalent (haploid); ER, exceeding rate; *n*, number of cases.

obtained high score values, despite a low 5 *c* ER. In contrast, agreement was achieved in low grade dysplasia with low scores and low 5 *c* ER, as well as in high grade dysplasia with high scores and high frequency of endoreplication. The correlation coefficient was $r_1 = 0.153$ and $r_2 = 0.533$ in low grade dysplasia and high grade dysplasia, respectively.

Chromosome division figures

The distribution and quality of CDFs were investigated through tumorigenesis. The 4.5 *c* ER of CDFs (Figure 2(a),(c),(e)) and their 5 *c* ER (Figure 2(b),(d),(f)) were compared with the 5 *c* ER of interphase nuclei. A high percentage of CDFs with > 4.5 *c* was found in low grade dysplasia, including even a few CDFs with > 5 *c* DNA. The DNA content of 7 remaining division figures was compatible with the mitotic range (Figure 2(a),(b)). In high grade dysplasia, 15 of 22 samples showed CDFs with > 5 *c* DNA (Figure 2(d)). The DNA content of CDFs increased with spreading endoreplication in interphase nuclei (Figure 2(c),(d)). The progression of DNA amplification in CDFs and endoreplication in interphase nuclei continued in cases of Ca (Figure 2(e),(f)).

With regard to DNA content, only mitotic 4.0 *c* figures but no CDFs were found in normal colon mucosa or with slight inflammation. The 4.5 *c* ER was only 1.0% of CDFs in Col, but 23.6% in low grade dysplasia, 43.2% in high grade dysplasia, and reached 61.0% in Ca (Table 3). Since the CDFs had been morphologically addressed (mad) before DNA measurement, *mad*-prophases, *mad*-metaphases and *mad*-telophases were discriminated and counted. The relative loss of *mad*-telophases in precancerous and cancerous lesions was a striking result (Table 3). The distribution profile of DNA

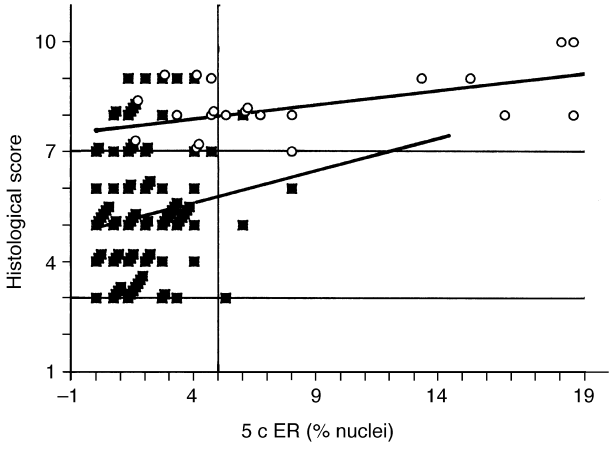

Figure 1. Intra-observer variation between histological scores. A first score was reported as LGD (93 specimens; squares) and HGD (22; circles). The second score was plotted to the 5 *c* ER from interphase nuclei. Agreement was 86.0% in low grade dysplasia and 81.8% in high grade dysplasia. Correlation for low grade dysplasia was $r_1 = 0.153$ ($y = 0.175x + 4.952$); high grade dysplasia $r_2 = 0.533$ ($y = 0.076x + 7.613$). Disagreement occurred at the histological transition from low grade dysplasia to high grade dysplasia.

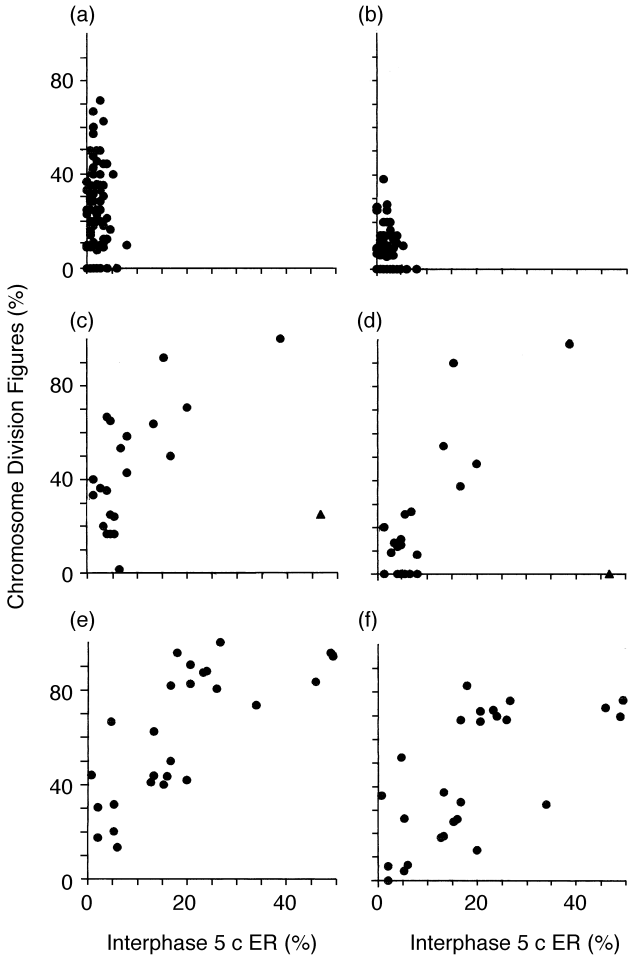

Figure 2. DNA content of CDFs compared with that of interphase nuclei in low grade dysplasia (a, b), high grade dysplasia (c, d), and Ca (e, f). Each point represents one case showing the 5 *c* ER of 150 interphase nuclei. The frequency of the corresponding CDFs was plotted either as 4.5 *c* ER (a, c, e) or 5 *c* ER (b, d, f). One runaway section for CDFs (triangle in (c) and (d)).

Table 3. DNA content and morphology of chromosome division figures (CDFs)

Histology	n_1	4.5 *c* ER (%)	5 *c* ER (%)	n_2	P (%)	M (%)	T (%)
Normal mucosa	5	0	0	473	37.8	34.7	27.5
Bacterial colitis	34	1.0 ± 0.8	0.2 ± 0.2	322	37.3	46.6	16.1
Low grade dysplasia	93	23.6 ± 1.8	5.5 ± 0.9	850	51.0	36.4	12.6
High grade dysplasia	22	43.2 ± 5.5	22.0 ± 6.0	246	44.3	39.8	15.9
Colon adenocarcinoma	26	61.0 ± 4.9	43.0 ± 4.9	853	53.0	38.3	8.7

Each entire CDF was measured from each case in 15 μm sections. Numerical scatter (±) given as standard error of the mean; n_1, number of samples; n_2 number of chromosome division figures (CDFs). The relative loss of telophases in Ca is a striking result. P, prophase; M, metaphase; T, telophase; addressed by their microscopic morphology.

content in CDFs was also monitored through tumorigenesis (Figure 3). True mitotic figures with regard to the DNA content of prophases, metaphases and both hemispheres of telophases were displayed within the 4 *c* peaks from Col, low grade dysplasia, high grade dysplasia and Ca. Progressive flattening of the distribution profile was caused by aberrant amounts of DNA, when more and more CDFs left the 4 *c* level. Thus, a reduction was observed from 51.9% mitoses with distinct 4.0 *c* DNA in Col (total 322 figures) to 31.5% in low grade dysplasia (850), 21.5% in high grade dysplasia (246) and 11.7% in Ca (853). Correspondingly, the percentage of CDFs > 6 *c* DNA was zero in Col, 0.2% in low grade dysplasia, 7.7% in high grade dysplasia and 21.6% in Ca.

Morphology of CDFs

The estimation of DNA content with pure light microscopy is not only difficult with interphase nuclei. With CDFs, in particular, an investigator could be misled by his expectation of 4 *c* values for mitotic figures. Therefore, morphology gives little support in discriminating CDFs from mitotic events. However, single cell microphotometry revealed that CDFs > 4 *c* were generally found in the vicinity of endoreplicated interphase nuclei. The shape and chromatic density of mitotic divisions showed only slight variation in Col (Figure 4(a),(b),(c)), compared to CDFs in high grade dysplasia (Figure 4(d),(e),(f)). Obvious enlargement of CDFs in Ca makes morphological discrimination from mitoses somewhat easier but not absolutely certain (Figure 4(g),(h),(i)).

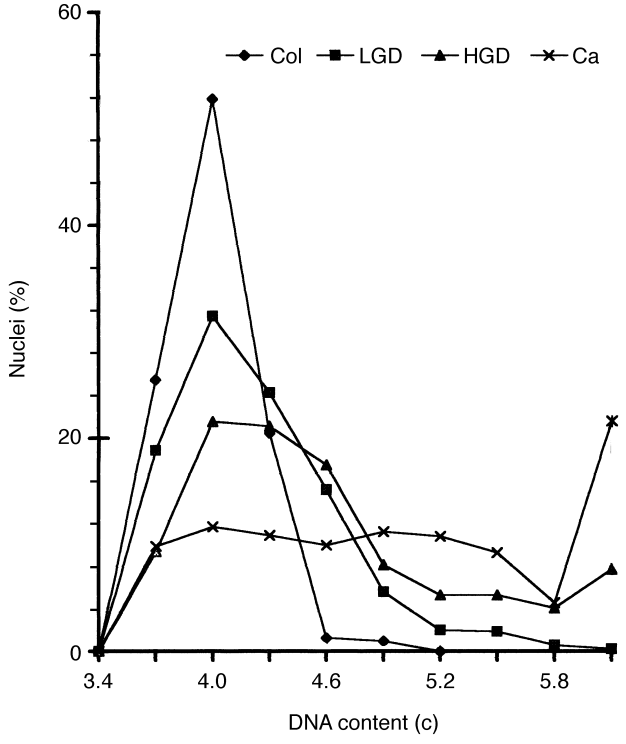

Figure 3. DNA distribution profiles of mitoses and CDFs in 15 μm sections. The transition from Col ($n = 322$), low grade dysplasia ($n = 850$), high grade dysplasia ($n = 246$) and Ca ($n = 853$) was characterised by a relative loss of mitoses with plain 4.0 *c* DNA content. The shift towards increased amounts of DNA in CDFs reflected genomic instability.

DISCUSSION

Subjectivity, precision and biological bias

Since multistep tumorigenesis is an accepted genetic model for colonic cancer [18], the histological score for low grade dysplasia and high grade dysplasia was designed mainly to evaluate nuclear features (Table 1). Changes and final damage of tissue architecture as well as coherent functions are secondary events related to long-standing ulcerative colitis. Intra-observer variation is a common problem in diagnostic routine and can be reduced by using a score [17, 19]. Generally, variation is negligible when the morphological feature heavily deviates from healthy tissue. However, look-alike lesions may give different results. The histological score, plotted against the results of a highly precise single-cell measurement, reflects low reliability when low grade dysplasia and high grade dysplasia of ulcerative colitis have a common borderline. Nuclei with similar appearance may possess rather different amounts of Feulgen DNA, because the volume increases with the power of 3 of the radius. In contrast, high reliability was achieved in clear-cut cases with pronounced nuclear atypia in high grade dysplasia and slight nuclear changes in low grade dysplasia (Figure 1).

The diagnostic reliability depends on the acquisition of a representative specimen by the operator. Here, the quality of the specimens and the measuring technique is reflected. Whole nuclei were achieved in sufficiently deep sections, 8 μm for interphase nuclei or 15 μm for mitoses and CDFs [14].

Frequency distributions of DNA content from interphase nuclei were recorded in low grade dysplasia and high grade dysplasia in ulcerative colitis and from Ca. Cases of normal and inflamed colon mucosa were added as representatives of the mitotic cell cycle (Table 2). Repeated measurements of the same nucleus indicated high precision, with a coefficient of variation (c.v.) of < 0.03 (not shown). The c.v. was 0.03 in diploid nuclei of normal mucosa, corroborating the precision of the measuring procedure. This scattering was similar to

that from pyogenic granuloma with c.v. = 0.05 from prophases, metaphases as well as both hemispheres of telophases [10]. Therefore, c.v. = 0.12 in the diploid nuclear population from low grade dysplasia, c.v. = 0.60 from high grade dysplasia and c.v. = 2.04 from Ca proved the biological bias of tumorigenesis. Increasing numerical scattering was correlated to the decrease in the diploid fraction of interphase nuclei from 94.3% in normal mucosa to 7.4% in Ca. This dramatic shift from the 2 *c* status to the 4 *c* level is probably caused by lagging prophase signals and by nuclei which missed mitotic division and entered DNA endoreplication. Thus, genomic instability became evident when the 5 *c* ER was zero in interphase nuclei of normal mucosa, 1.9% in low grade dysplasia, 10.3% in high grade dysplasia, and 20.5% in Ca (Table 2).

Mitotic figures, endoreplication and CDFs

Mitotic activity is generally studied in cytogenetic spreads after *in vitro* culturing. In contrast, mitotic figures are rather rare or absent in samples of smears, fine-needle aspiration or imprints from human lesions. Even in frozen sections from advanced malignancies, mitotic figures are missed, probably due to etching artifacts. Therefore, the role of mitosis has attracted little attention *in vivo*, when tissues have entered a

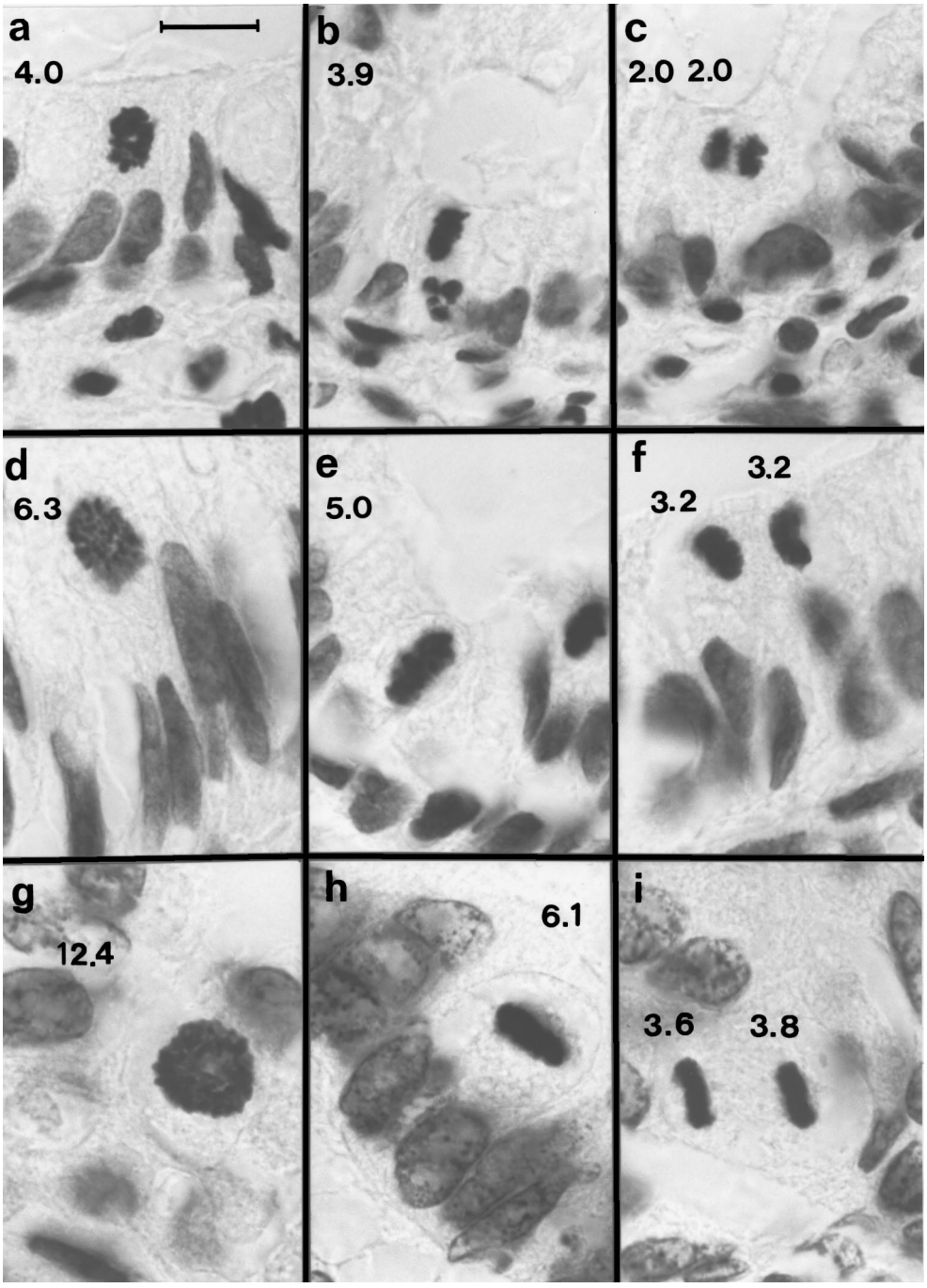

Figure 4. Examples of CDFs. Bacterial colitis is illustrated in (a–c), high grade dysplasia in (d–f) and cancer in (g–i). Prophases (a, d, g), metaphases (b, e, h) and telophases (c, f, i). Bar represents 10 μm.

precancerous status. Paraffin-embedded material forms the exception, allowing the observation of all cell-cycle events *in situ*. Precancerous conditions provide a promising target of investigation and can best be exploited when descriptive microscopy is supplemented by single-cell quantitation. Ordinary nuclear divisions need space for anaphase movement and telophase distribution. Therefore, in our study, the thickness of sections was increased from 8 to 15 μm.

DNA deviations from the mitotic range have been recorded in interphase nuclei with the onset of microphotometry [20–23]. These nuclei, hyperchromatic from their morphology, begin further S-phase(s) in the absence of karyokinesis. Since their DNA content (> 4 *c*) frequently does not match plain *c* values, the term DNA aneuploidy has been coined to address the peculiar distribution profiles (histograms) from these nuclear populations. Both the redundant S-phase(s) and the distribution between DNA classes have been covered by the term DNA endoreplication instead of endoreduplication [10]. It was surprising that morphologically addressed (*mad*-) division figures left the mitotic range in correlation with the progress of the lesion. Thus, the 5 *c* ER was 5.5% in low grade dysplasia, but 22.0% in high grade dysplasia and 43.0% in Ca (Table 3). CDFs and aberrant interphase nuclei were positively correlated (Figure 2). In low grade dysplasia, the CDFs showed a 5 *c* ER up to 40% (Figure 2(b)), whereas the 5 *c* ER averaged 0.2% in Col (Table 3). Since the CDFs showed a profile which was characteristic for DNA aneuploidy with interphase nuclei, the triggers for chromosome condensation (*mad*-prophase), equatorial aggregation (*mad*-metaphase) and segregation (*mad*-telophase) were probably delayed. If this is true, the delayed prophase should arrest the re-initiated origins at multiple chromosomal replicons [24, 25] or should interrupt their elongation. Uncoupling of the S-phase from mitosis produces endoreplicated nuclei [8]. Repeated rounds of DNA replication have been observed in the absence of mitosis when fission yeast cells overexpressed the *rum1* gene, acting as an inhibitor of the cdc2/cyclin B complex [26]. Likewise, the overexpression of *cdc18* or the deletion of *cdc13*, which encodes the major B cyclin in fission yeast, induces re-replication [27].

The CDFs with aberrant amounts of DNA are different from endomitoses, which are considered to be cases of real genome multiplication due to chromosome counts [4, 9]. Redundant DNA contents have been discussed in several cases of local amplification of clustered long-range repeats in homogeneously staining regions [28–31]. Recently, additional nuclear DNA has been detected by 2-D gel electrophoresis of HeLa cells and colon carcinoma where a rolling circle mechanism has been discussed [32]. However, such small amounts of DNA cannot be detected by microphotometry. Mitelman [33] has shown that cytogenetic aneuploidy dominates cell nuclei in tumours. Furthermore, chromosomal non-disjunction could evoke unequal amounts in *mad*- telophases (Figure 4(i)). The CDFs possessing 6.3 *c* and 12.4 *c* DNA (Figure 4(d),(g)) raise a further possibility that only one genome was multiplied and the other was 'silent' [34]. The morphology of compacted CDFs provides evidence that DNA elimination [35–37] does not play a role in DNA aneuploidy with human tumours. The complex distribution profile of DNA aneuploidy might be enhanced by the progeny of aberrant anaphases and telophases. It is unlikely that only a one-factor mechanism is responsible for DNA aneuploidy, and molecular approaches will clarify this question. In any case, the transformation schedule described at the cellular level is not restricted to ulcerative colitis, but is also valid with precancerous conditions in the oral cavity, stomach, colon, cervix uteri and skin. These lesions are known to develop into carcinomas with severe DNA aneuploidy.

Multistep progress: molecular defects and morphological effects

The favoured model for colorectal tumorigenesis has been proposed by Vogelstein. A possible alteration of the *MCC* gene (mutated in colon cancer) on chromosome 5q might provoke an abnormal proliferation of a colon cell [18, 38]. The onset of morphological changes can be described by budding and branching of the crypts [15]. This enhanced cellular proliferation produces a higher number of cells and shifts the proportion between committed and apoptotic cells. It demands enlargement of the basement membrane and forms additional transverse crypts (budding). Further cellular proliferation of the new crypts results in their branching (Table 1). Early genetic alterations have been traced with comparative genomic hybridisation [13] and their linkage to morphological phenotypes has become obvious from numerous CDFs (unpublished data). Here, early rising CDFs were shown in low grade dysplasia (Figure 2(a),(b)). CDFs in telophase reveal unequal divisions, probably caused by non-disjunction and/or chromosome breakage.

Additional mutations of the gene complex, which regulates the transition from G_1 to S-phase, are linked with entry in DNA endoreplication leading to hyperchromatic and enlarged interphase nuclei and a corresponding increase in the 5 *c* ER of CDFs. These alterations are consistent with high grade dysplasia (Figures 2 and 3; Table 1).

Further mutations (e.g. in the *DCC* gene, deleted in colon cancer, on 18q) [38] and clonal selection [39] may strengthen a long-standing ulcerative colitis. The transition from advanced, dysplastic ulcerative colitis with a villous, adenomatous or tubular pattern (Table 1) to carcinoma is often accompanied, and perhaps driven, by mutation of the *p*53 gene on 17p. The effect of clonal selection in tumorigenesis was obvious from a relative decrease in the number of *mad*-telophases (Table 3). Tumour progress revealed a loss of the 4.0 *c* peak from mitotic figures, while the increasing frequency of CDFs flattens the distribution profile of DNA content (Figure 3). The data suggest that the average DNA increase of CDFs should be used to follow up long-standing ulcerative colitis. Since the nuclear DNA content is an objective and reproducible parameter, it is useful for the two-level classification of ulcerative colitis.

1. Moum B, Vatn MH, Ekbom A, *et al.* Incidence of ulcerative colitis and intermediate colitis in four counties of southeastern Norway, 1990–93. *Scand J Gastroenterol* 1996, **31**, 362–366.
2. Sandritter W. Methods and results in quantitative cytochemistry. In Wied GL, ed. *Introduction to Quantitative Cytochemistry*, vol 1. New York, Academic Press, 1966, 159–181.
3. Ploem-Zaaijer JJ, Beyer-Boon ME, Leyte-Veldstra L, Ploem JS. Cytofluorometric and cytophotometric DNA measurements of cervical smears stained using a new bicolor method. In Pressmann NJ, Wied GL, eds. *Automation of Cancer Cytology and Cell Image Analysis*. Chicago, Tutorials of Cytology, 1979, 225–235.
4. Hiddemann W, Schumann J, Andreeff M, *et al.* Convention on nomenclature for DNA cytometry. *Cytometry* 1984, **5**, 445–446.
5. Geitler L. Endomitose und endomitotische Polyploidisierung. In Heilbrunn LV, Weber F, eds. *Protoplasmatologia*, vol 6c. Wien, Springer, 1953.

6. Nagl W. *Endopolyploidy and Polyteny in Differentiation and Evolution*. Amsterdam, Elsevier, 1978.
7. Brodsky VY, Uryvaeva IV. Genome multiplication in growth and development. Biology of polyploid and polytene cells. In Barlow PW, Green PB, Wylie CC, eds. *Developmental and Cell Biology Series*. Cambridge, Cambridge University Press, 1985.
8. Waldman T, Lengauer C, Kinzler KW, Vogelstein B. Uncoupling of S phase and mitosis induced by anticancer agents in cells lacking p21. *Nature* 1996, **381**, 713–716.
9. Geitler L. Die Entstehung der polyploiden Somakerne der Heteropteren durch Chromosomenteilung ohne Kernteilung. *Chromosoma* 1939, **1**, 1–22.
10. Steinbeck RG. Atypical mitoses in lesions of the oral mucosa: A new interpretation of their impact upon tumorigenesis. *Oral Oncol* 1997, **33B**, 110–118.
11. Oksala T, Therman E. Mitotic abnormalities and cancer. In German J, ed. *Chromosomes and Cancer*. New York, Wiley & Sons, 1974, 239–263.
12. Therman E, Susman M. *Human Chromosomes: Structure, Behavior, and Effects*, 3rd edn. Berlin, New York, Springer, 1993.
13. Ried T, Knutzen R, Steinbeck R, *et al.* Comparative genomic hybridization reveals a specific pattern of chromosomal gains and losses during the genesis of colorectal tumors. *Genes Chromosomes Cancer* 1996, **15**, 234–245.
14. Klapperstück T, Wohlrab W. DNA image cytometry on sections as compared with image cytometry on smears and flow cytometry in melanoma. *Cytometry* 1996, **25**, 82–89.
15. Morson BC. Precancer and cancer in inflammatory bowel disease. *Pathology* 1985, **17**, 173–180.
16. Steinbeck RG. Proliferation and DNA aneuploidy in mild dysplasia imply early steps in cervical carcinogenesis. *Acta Oncol* 1997, **36**, 3–12.
17. Steinbeck RG, Heselmeyer KM, Neugebauer WF, Falkmer UG, Auer GU. DNA ploidy in human colorectal adenocarcinomas. *Anal Quant Cytol Histol* 1993, **15**, 187–194.
18. Vogelstein B, Kinzler KW. The multistep nature of cancer. *Trends Genet* 1993, **9**, 138–142.
19. Anneroth G, Hansen LS. A methodological study of histologic classification and grading of malignancy in oral squamous cell carcinoma. *Scand J Dent Res* 1984, **92**, 448–468.
20. Sandritter W. Über den Nukleinsäuregehalt in verschiedenen Tumoren. *Frankf Z Pathol* 1952, **63**, 422–446.
21. Atkin NB, Richards BM. Deoxyribonucleic acid in human tumours as measured by microspectrophotometry of Feulgen stain: A comparison of tumours arising at different sites. *Br J Cancer* 1956, **10**, 769–786.
22. Caspersson T, Lomakka G, Caspersson O. Quantitative cytochemical methods for the study of tumor cell populations. *Biochem Pharmacol* 1960, **4**, 113–127.
23. Caspersson O. Quantitative cytochemical studies on normal, malignant, premalignant and atypical cell populations from the human uterine cervix. *Acta Cytol* 1964, **8**, 45–60.
24. Huberman JA, Riggs AD. Autoradiography of chromosomal DNA fibers from Chinese hamster cells. *Proc Natl Acad Sci USA* 1966, **55**, 599–606.
25. Callan HG. Replication of DNA in the chromosomes of eukaryotes. *Proc R Soc B (Lond)* 1972, **181**, 19–41.
26. Moreno S, Nurse P. Regulation of progression through the G_1 phase of the cell cycle by the rum1$^+$ gene. *Nature* 1994, **367**, 236–242.
27. Nishitani H, Nurse P. p65–cdc18 plays a major role controlling the initiation of DNA replication in fission yeast. *Cell* 1995, **83**, 397–405.
28. Balaban-Malenbaum G, Grove G, Gilbert F. Increased DNA content of HSR-marker chromosomes of human neuroblastoma cells. *Exp Cell Res* 1979, **119**, 419–423.
29. Kury F, Slintz G, Schemper M, *et al.* HER-2 oncogene amplification and overall survival of breast carcinoma patients. *Eur J Cancer* 1990, **26**, 946–949.
30. Schimke RT, Brown PC, Kaufman RJ, McGrogan M, Slate DL. Chromosomal and extrachromosomal localization of amplified dihydrofolate reductase genes in cultured mammalian cells. *Cold Spring Harbor Symp Quant Biol* 1981, **45**, 785–796.
31. Alitalo K, Schwab M, Lin CC, Varmus HE, Bishop JM. Homogeneously staining regions contain amplified copies of an abundantly expressed cellular oncogene (c-myc) in malignant neuroendocrine cells from a human colon carcinoma. *Proc Natl Acad Sci USA* 1983, **80**, 1707–1711.
32. Cohen S, Regev A, Lavi S. Small polydispersed circular DNA (spcDNA) in human cells: association with genomic instability. *Oncogene* 1997, **14**, 977–985.
33. Mitelman F. *Catalog of Chromosome Aberrations in Cancer*, 5th edn. New York, Wiley-Liss, 1994.
34. Nur U. Nonreplication of heterochromatic chromosomes in a mealy bug, *Planococcus citri* (Coccoidea: Homoptera). *Chromosoma* 1966, **19**, 439–448.
35. Beermann S. The diminution of heterochromatic chromosomal segments in Cyclops (Crustacea, Copepoda). *Chromosoma* 1977, **60**, 297–344.
36. Kubota S, Kuro-o M, Mizuno S, Kohno S. Germ line-restricted, highly repeated DNA sequences and their chromosomal localization in a Japanese hagfish (*Eptatretus okinoseanus*). *Chromosoma* 1993, **102**, 163–173.
37. Esteban MR, Giovinazzo G, Goday C. Chromatin diminution is strictly correlated to somatic cell behavior in early development of the nematode *Parascaris univalens*. *J Cell Sci* 1995, **108**, 2393–2404.
38. Vogelstein B. Genetic alterations in colorectal tumors. *Adv Oncol* 1993, **7**, 3–6.
39. Nowell PC. The clonal evolution of tumor cell populations. *Science* 1976, **194**, 23–28.

Acknowledgements—Professor Gert Auer, Department of Oncology and Pathology, Karolinska Institute, Stockholm, has provided part of research facilities. Mr Uwe Koester, Flensburg, has given excellent technical assistance. Ms Jayne Welling-Wolf, Kiel (Germany), provided linguistic aids. Supported by the Swedish Cancer Society, Stockholm, and the Research Funds of the Institute of Pathology, Flensburg (Germany).